The Journal of Immunology

Interaction of Streptavidin-Based Peptide–MHC Oligomers (Tetramers) with Cell-Surface TCRs

Jennifer D. Stone, Maxim N. Artyomov, Adam S. Chervin, Arup K. Chakraborty, Herman N. Eisen and David M. Kranz

J Immunol 2011; 187:6281-6290; Prepublished online 18 November 2011;
doi: 10.4049/jimmunol.1101734
http://www.jimmunol.org/content/187/12/6281

The Journal of Immunology is published twice each month by
The American Association of Immunologists, Inc.,
1451 Rockville Pike, Suite 650, Rockville, MD 20852

Print ISSN: 0022-1767 Online ISSN: 1550-6606.

Interaction of Streptavidin-Based Peptide–MHC Oligomers (Tetramers) with Cell-Surface TCRs

Jennifer D. Stone,*[,1] Maxim N. Artyomov,[†,‡,§,¶,1] Adam S. Chervin,* Arup K. Chakraborty,[†,‡,§,¶] Herman N. Eisen,[‖,#] and David M. Kranz*

The binding of oligomeric peptide–MHC (pMHC) complexes to cell surface TCR can be considered to approximate TCR–pMHC interactions at cell-cell interfaces. In this study, we analyzed the equilibrium binding of streptavidin-based pMHC oligomers (tetramers) and their dissociation kinetics from CD8^{pos} T cells from 2C-TCR transgenic mice and from T cell hybridomas that expressed the 2C TCR or a high-affinity mutant (m33) of this TCR. Our results show that the tetramers did not come close to saturating cell-surface TCR (binding only 10–30% of cell-surface receptors), as is generally assumed in deriving affinity values (K_D), in part because of dissociative losses from tetramer-stained cells. Guided by a kinetic model, the oligomer dissociation rate and equilibrium constants were seen to depend not only on monovalent association and dissociation rates (k_{off} and k_{on}), but also on a multivalent association rate (μ) and TCR cell-surface density. Our results suggest that dissociation rates could account for the recently described surprisingly high frequency of tetramer-negative, functionally competent T cells in some T cell responses. ***The Journal of Immunology*****, 2011, 187: 6281–6290.**

Because Abs and many Ags are soluble, it has been possible to study their interactions with a variety of methods under conditions that are physiological or nearly so. For TCRs and their peptide–MHC (pMHC) ligands, however, their natural state as integral membrane proteins on T cells and APCs limits the options for analyzing their interactions. Considerable insights have been gleaned from responses of T cells to pMHC displayed at various levels on other cells (target cells or APCs). The responses are informative particularly when correlated with measurements of equilibrium constants and reaction rates, but the latter are most often determined with rTCR and MHC molecules in the absence of CD8 and CD4 coreceptors. Because these coreceptors have a pronounced impact on the cellular responses, efforts have been made to study the binding of soluble pMHC complexes to TCR on intact CD8^{pos} T cells (1). As monomers, these complexes are of limited use because they dissociate too rapidly from TCR (2, 3). However, pMHC oligomers bind more stably. Hence, they are widely used to identify T cells with cognate TCR and also, though much less widely, to determine TCR–pMHC affinities and reaction rates. The oligomeric forms include IgG dimers (4) and pentamers (ProImmune, Oxford, U.K.), but most often, as in the current study, streptavidin (SA)-linked pMHC oligomers, called tetramers (5–7), as originally introduced by Altman et al. (8).

It has been generally accepted that the proportion of T cells that are stained by chromophore-labeled tetramers accurately measures the frequency of T cells that express the corresponding (cognate) TCRs. There are reports, however, of CD8$^+$ T cells that respond specifically to pMHC on target cells, yet are not stained by the same pMHC as tetramers (9–12). Recently, a surprisingly high frequency of CD4$^+$ T cells that are similarly tetramer-negative but functionally competent has been described in responses to infection by lymphocytic choriomeningitis virus and especially to a self-antigen [myelin oligodendrocyte glycoprotein (13)].

Studies have shown that the intensity of tetramer staining of T cells generally correlates with monovalent TCR–pMHC affinity and several other variables, including the density of TCR on T cells, lipid membrane organization, and differentiation status of the cells [activated versus naive T cells (12, 14–18)]. Estimates of the multivalent affinity (avidity) of cell surface TCR for tetramers are taken as the concentration of free tetramer at half-maximal binding of tetramer to cells, a determination that assumes saturation of surface TCR by bound tetramers at high free tetramer concentration. This assumption was questioned by a recent study (19), in which a panel of TCR that differed widely in affinity for the same pMHC was expressed in hybridomas that were stained with that pMHC in tetrameric form. Although the TCR levels were expressed at the same levels in all hybridomas, the maximal levels of tetramer staining varied considerably, raising the possibility that cell surface TCR were not saturated in any of the cells tested.

To evaluate this possibility, we analyzed in this study the equilibrium binding of pMHC tetramers and their dissociation kinetics from CD8^{pos} T cells from 2C TCR-transgenic mice and transduced T cell hybridomas that expressed the 2C TCR (20) or an engineered high-affinity mutant [m33 (21)] of this TCR. The analyses were based on a kinetic model of multimeric pMHC binding to cell surface TCR. The results establish that tetramers

*Department of Biochemistry, University of Illinois, Urbana-Champaign, Urbana, IL 61801; [†]Department of Chemical Engineering, Massachusetts Institute of Technology, Cambridge, MA 02139; [‡]Department of Chemistry, Massachusetts Institute of Technology, Cambridge, MA 02139; [§]Department of Biological Engineering, Massachusetts Institute of Technology, Cambridge, MA 02139; [¶]Ragon Institute of MGH, MIT, and Harvard, Cambridge, MA 02129; [‖]The David H. Koch Institute for Integrative Cancer Research, Massachusetts Institute of Technology, Cambridge, MA 02139; and [#]Department of Biology, Massachusetts Institute of Technology, Cambridge, MA 02139

[1]J.D.S. and M.N.A. contributed equally to this work.

Received for publication June 14, 2011. Accepted for publication September 30, 2011.

This work was supported by National Institutes of Health Grants P01 CA097296, R01 GM55767 (to D.M.K.), and PO1-AI071195, a National Institutes of Health's Director's Pioneer award (to A.K.C.), a Cancer Center Core grant (to T. Jacks for H.N.E.), and a Samuel and Ruth Engelberg/Irvington Institute fellowship of the Cancer Research Institute (to J.D.S.).

Address correspondence and reprint requests to Dr. Jennifer D. Stone, Department of Biochemistry, University of Illinois, Urbana-Champaign, 600 S. Mathews Avenue, Urbana, IL 61801. E-mail address: jstone@illinois.edu

The online version of this article contains supplemental material.

Abbreviations used in this article: 2D, two-dimensional; pMHC, peptide–MHC; scTCR, single chain Vβ-linker-Vα TCR; SPR, surface plasmon resonance.

www.jimmunol.org/cgi/doi/10.4049/jimmunol.1101734

did not come close to saturating cell-surface TCR, in part because of their dissociation when tetramer-stained cells are washed. Besides the intrinsic (monovalent) association and dissociation rates, critical determinants of tetramer dissociation are the multivalent association rate (μ) and the two-dimensional (2D) concentration (density) of cell-surface TCR. The rapidity of dissociation of tetramers from some TCR can account for the frequency of tetramer-negative, functionally competent T cells.

Materials and Methods

Peptides, Abs, and cells

SIY (SIYRYYGL) and OVA (SIINFEKL) peptides were synthesized by the Macromolecular Core Facility of the Section of Research Sources, Penn State College of Medicine. Peptides were purified by reverse phase chromatography using a C-18 column, and masses were confirmed by MALDI. Peptide quantification by amino acid analysis was performed at the Molecular Structure Facility, University of California, Davis (Davis, CA).

Fluorescein-labeled mAbs (F23.1, H57-597, 145-2C11, 53-6.7, and 53-5.8) and SA were purchased from BD Pharmingen (San Jose, CA). The 1B2 anti-2C TCR and B.8.24.3 anti-K^b mAbs were purified from hybridoma supernatant using protein G beads. 1B2 was labeled with FITC, and purified to remove excess FITC. For each fluorescein-labeled protein, the protein concentration and number of fluorescein molecules per protein molecule was determined by comparing the ratio of UV-Vis absorbance at 495 nm and 280 nm (PBS [pH 7.4]), using a molar extinction coefficient of 69,000 for fluorescein at 495 nm, and subtracting $0.2 \times A_{495}$ from the absorbance at 280nm to yield protein absorbance and concentration. Multiple independent dilutions of each protein were scanned to determine the fluorescein to protein ratio. Protein molar extinction coefficients were taken as ε_{280} = 176,000 for SA, and ε_{280} = 210,000 for Abs.

$58^{-/-}$ T cell hybridomas retrovirally transduced with various TCR genes, with or without coexpression of CD8$\alpha\beta$, were maintained in RPMI-1640 supplemented with 10% FCS, L-glutamine, penicillin and streptomycin. Splenic T cells from 2C TCR transgenic mice on a $RAG^{-/-}$ background or from C57BL/6 mice were purified by negative selection of non-T cells with magnetic beads (Dynal, Invitrogen, Carlsbad, CA). Differential interference contrast microscopy was performed using an Olympus BX51 microscope, and cell size measurements were made using the Microsuite software (Olympus America, Center Valley, PA).

Protein expression and preparation

Single chain Vβ-linker-Vα TCR (scTCR) were expressed as inclusion bodies in BL21(DE3) *Escherichia coli* (Stratagene, La Jolla, CA). The stable single chain 2C TCR that includes an interdomain flexible linker (22) has been previously shown to maintain binding specificity for all ligands tested, and binding measured by surface plasmon resonance (SPR) has shown identical binding affinity and kinetics for the scTCR and full length, soluble TCR without a linker (23, 24). Proteins were solubilized in urea and refolded by dilution as previously described (19). The refolded protein was purified by binding to Ni-NTA agarose beads (Qiagen, Valencia, CA), followed by elution in 500 mM imidizole, followed by size exclusion chromatography over a Superdex 200 gel filtration column (GE Healthcare, Piscataway, NJ).

H2-K^b H chain containing a C-terminal biotinylation signal peptide and human β2 microglobulin L chains were expressed separately in *E. coli*. H2-K^b H chain was biotinylated in vivo by coinduction of biotin ligase, so that the H chain carried a biotin tag (25). Both chains were expressed as inclusion bodies, solubilized in urea and refolded together in vitro in the presence of excess SIY or OVA peptide (19). Folded complexes were purified by anion exchange chromatography using HiTrap Q columns (GE Healthcare, Piscataway, NJ) and size exclusion chromatography. For incorporation of SIY/K^b into SA-oligomers, precharacterized, calibrated, fluorescein-labeled SA was added stepwise to the biotinylated SIY/K^b complexes in small aliquots on ice over 20 min to various final molar ratios. Characterization of the resulting oligomer complex distribution was performed by SDS-PAGE.

Binding measurements of soluble receptors at 10°C

Kinetic and equilibrium binding data were obtained by SPR using a BIAcore 3000 (Biacore Life Sciences, GE Healthcare, Piscataway, NJ) precooled to 10°C. Biotinylated SIY/K^b and OVA/K^b monomers were immobilized on a neutravidin-coated CM5 sensor chip on different flow cells to ~400 response units. Soluble scTCRs were purified by size-exclusion chromatography not >24 h before making measurements to avoid aggregates. The scTCRs were flowed over the SIY/K^b and OVA/K^b at various concentrations in Biacore buffer (20 mM HEPES, 150 mM NaCl, 3 mM EDTA, 0.005% Tween-20 [pH 7.4]; Biacore Life Sciences) at 30 μl/min. Binding of scTCRs to the null complex OVA/K^b was subtracted from TCR binding to SIY/K^b to correct for bulk shift and any nonspecific binding. On-rates, off-rates, and kinetic-based K_D analyses were performed using BIAEvaluation 3.0 software (Biacore Life Sciences).

Oligomer binding and dissociation experiments

To perform steady-state oligomer binding titrations, $58^{-/-}$ cells transduced with TCR genes (2C, m33, or other mutants) or T cells purified from 2C transgenic or C57BL/6 mouse splenocytes were incubated with various concentrations of fluorescein-labeled SA-SIY/K^b oligomers in FACS buffer (1% BSA in PBS with 0.02% sodium azide) on ice for at least 2 h in the dark. After an 8 min wash in cold (~10°C) FACS buffer, cells were resuspended in cold FACS buffer and analyzed for bound fluorescent tetramers by flow cytometry. Fluorescence levels of the parental $58^{-/-}$ cell line (control) were subtracted as background from the TCR transfected hybridoma values at the same staining concentration.

Oligomer dissociation experiments were performed as described previously (19, 26–28). Briefly, $58^{-/-}$ cells transfected with mutant TCR chains or 2C TCR transgenic T cells purified from mouse splenocytes were stained with 293 nM (or 5.85 μM for 2C TCR hybridomas without CD8$\alpha\beta$) SA-linked SIY/K^b tetramers on ice for 2 h. Cells were washed and resuspended in 25°C dissociation buffer containing 2% FCS, 0.1% azide, 100 μM cytochalasin D, and 200 μg/ml K^b-blocking Ab (B.8.24.3, to prevent rebinding) in RPMI-1640. At various times, cells were diluted in ice-cold PBS containing 1% BSA and 0.02% azide and analyzed by flow cytometry. Complete dissociation was determined to be the level of staining observed for the parental $58^{-/-}$ cell line or for C57BL/6 cells. Data from dissociation experiments were fit by an equation describing a first-order exponential decay.

Quantification of cell surface-bound Abs and oligomers

Cells were stained at 4°C in the dark with saturating amounts of calibrated fluorescein-labeled Abs (determined by titration), or the indicated levels of SIY/K^b oligomer made with calibrated fluorescein-labeled SA, for at least 2 h. The cells were then washed for 8 min at 4°C in a large excess of FACS buffer, and resuspended immediately prior to analysis by flow cytometry (FACS Canto, BD Biosciences, San Jose, CA). Quantification of molecules per cell was derived from flow cytometry experiments in which specific fluorescence was analyzed in relation to calibrated fluorescein beads (Spherotech, Lake Forest, IL and Bangs Labs, Fishers, IN, Supplemental Figs. 1, 2). Fluorescent beads were analyzed at the same cytometer settings as the stained cells, and measured fluorescence values were used to convert corrected cell-bound fluorescence to numbers of cell-bound fluorescein-molecule equivalents. These latter values were used to calculate the number of cell-bound Ab molecules or SA-oligomers.

Model

To describe the behavior of SA-linked oligomers binding to and dissociating from T cells, we developed and applied a quantitative model. As the oligomers used in this study have on average three pMHC complexes per SA molecule (Fig. 1*A*, below), our model assumes that an SA-oligomer can bind to one, two, or three cell-surface TCR molecules; these various bound states are described as $L - T$, $L = T$, and $L \equiv T$, where L refers to oligomer (ligand) and T to TCR. As discussed below (in *Results*) and shown in detail in Appendix A: Model Equations, a bound oligomer's effective dissociation rate (k_{off}^{eff}) is determined by two parameters: k_{off} (the intrinsic dissociation rate of the pMHC–TCR bond, as measured, for example, by SPR) and μ (a multivalent k_a with units of s^{-1}, which is related to the intrinsic [univalent] pMHC–TCR association rate, k_{on} [with units of $M^{-1}s^{-1}$], and an effective concentration of surface T, as discussed below in *Results*).

At equilibrium, the oligomer association and dissociation rates are equal, as described by: $k_{on}^{'} T_{free} \cdot L_{sol} = k_{off}^{eff} L_{bound}$, where $k_{on}^{'}$ is on-rate for the monomeric pMHC–TCR interaction, as measured for instance by SPR, modified by the number of pMHC per SA molecule. If θ is the fraction of occupied receptors, $T_{free} = (1 - \theta)T_{total}$, and $L_{bound} = \theta T_{total}$, we can express the ratio of bound to free receptors as Eq. 5, which resembles the Scatchard equation (29–31), then follows. Detailed derivation of the equilibrium equations (including Eq. 5) can be found in Appendix A: Model Equations.

In describing these multivalent binding events, we assume that a pseudo-equilibrium between the T cell-bound states of an oligomer is reached rapidly compared with the overall association or dissociation of an oligomer from the T cell. This assumption is justified where $\mu >> k_{off}$, as is the case

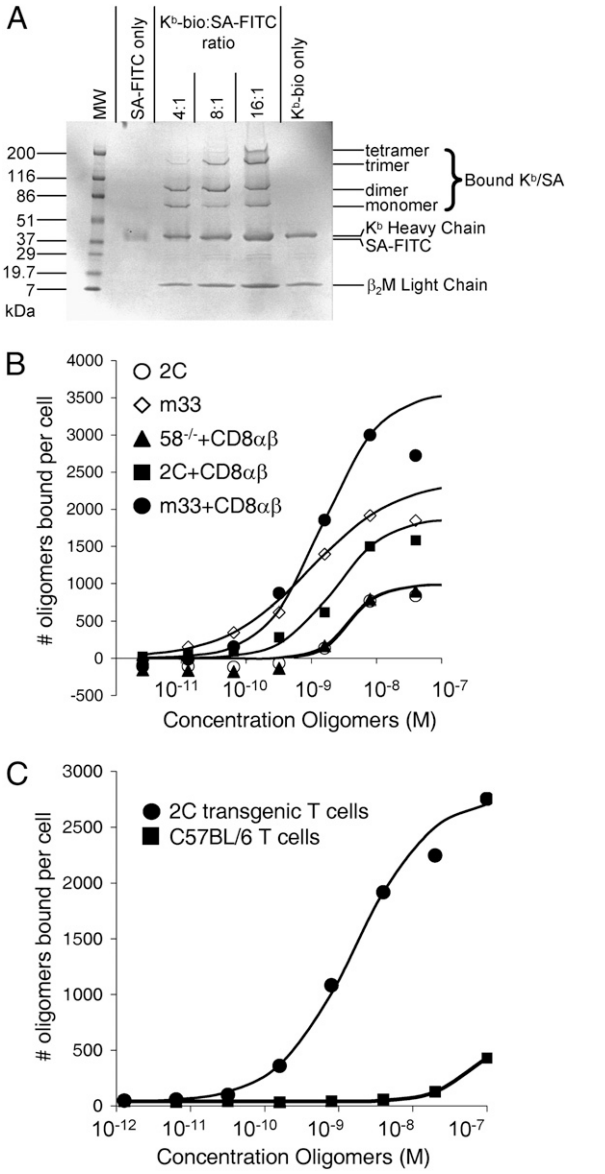

FIGURE 1. MHC oligomer staining of retrovirally-transduced T cell hybridomas. *A*, Distribution of oligomeric species in oligomer (tetramer) preparations. Reduced, unboiled gradient SDS-PAGE gel of reaction of different molar ratios of biotinylated H2-K^b and SA. The K^b is biotinylated site specifically on the H chain concurrently with translation by biotin ligase-expressing *E. coli*, with a modification efficiency of ~50%. The following experiments were carried out using reagent corresponding to 16:1 MHC:SA ratio. *B*, Steady-state oligomer staining of T cell hybridomas with and without CD8αβ expression—corrected by subtracting fluorescence of $58^{-/-}$ cells without TCR or CD8 at the same conditions. *C*, Steady-state staining of 2C transgenic T cells carried out at 4°C using various concentrations of SIY/K^b:SA-oligomer. Binding of SIY/K^b:SA-oligomer to C57BL/6 T cells was subtracted from binding to 2C transgenic T cells. Quantification of molecules per cell indicates number of fluorescent SAs associated with the cell; actual number of MHC-bound TCRs may be up to three times higher.

for the TCR–pMHC interactions described in this study (μ~10-40-fold larger than k_{off}). In addition, our interactions are in the range where dissociation data can be described by an exponential decay curve; a lack of rapid interconversion of bound states would result in a different shape to the dissociation data (32). In a range where this assumption is not valid, including much more weakly binding receptors, the amount of bound oligomer over time could be determined by numerically solving the set of differential equations defining the interactions in Appendix A: Model Equations (Eq. A1–A3). Moreover, with the assumption $\mu >> k_{off}$, k_{off}^{eff} can be obtained from Eq. 2 in the text, the derivation of which can be found in Appendix A: Model Equations.

In this model, we also assume no positive or negative cooperativity of binding, which could affect on-rates or off-rates beyond the statistical factors we have applied to μ and k_{off}. Although this assumption may not be fully accurate, there is no clear way to account for such effects. Based on the successful application of this model to our data, we suspect that any cooperativity, if present, does not affect our overall conclusions.

Results

Characterization of pMHC–SA-linked oligomers (tetramers)

The complexes formed by SA with biotinylated MHC, usually called tetramers, vary in the number of biotinylated MHC molecules per SA molecule (33, 34). Fig. 1*A* shows the distribution of oligomers when biotinylated class I MHC and SA were combined at different molar ratios. Based on these results, the preparations used for subsequent work (below) were, assembled with a 16:1 molar ratio of SIY/K^b:SA; they consisted of ~40% trimer, and 20% each tetramer, dimer, and monomer bound to SA. Because of the size distribution (Fig. 1*A*), we refer to them susequently as SA-oligomers, or simply oligomers, rather than as tetramers.

Analysis of steady-state binding of pMHC oligomers to T cells

To relate oligomer binding to TCR affinity, CD8 contribution, and cell surface levels of TCR and CD8, we first measured the steady-state binding of SIY/K^b oligomers to T cell hybridomas that expressed the 2C TCR (20) or an engineered, high-affinity mutant [m33 (21)] of this TCR (Fig. 1*B*), and also to naive CD8$^+$ 2C T cells freshly isolated from spleens of 2C TCR transgenic mice (Fig. 1*C*). CD8α and CD8β were coexpressed in some of the hybridomas. After the cells were incubated on ice for 2 h with oligomers at various concentrations, they were dispersed in a large volume of cold buffer, centrifuged, and the pelleted cells resuspended immediately before analysis by flow cytometry. The cell-bound oligomers increased with increasing free oligomer concentration to a maximum level and reached a plateau, or declined slightly, at the highest concentrations (Fig. 1*B*, 1*C*). The treatment used in this study is typical of oligomer staining protocols where binding is allowed to reach steady-state, and the cells are washed prior to analysis by flow cytometry. Although these data may be fit by a sigmoidal curve similar to equilibrium binding data giving a 50% maximum value ($K_{D,olig}$) that can be compared from cell population to cell population, this does not precisely correspond to a true equilibrium binding constant (see below). To obtain a more representative equilibrium on a cell surface, techniques such as spinning cells through oil rapidly to remove unbound ligands (1) or avoiding a wash step entirely (15) have been employed previously.

As shown in Fig. 1*B*, SIY/K^b oligomers bound equally well to 1) hybridoma cells ($58^{-/-}$) that expressed CD8 but not 2C TCR and 2) hybridoma cells that expressed the 2C TCR but not CD8. This finding is consistent with the similar binding constants found for the binding of CD8αβ to peptide-K^b [K_D = 38 μM (35)] and 2C TCR to SIY-K^b [K_D = 30 μM (19, 23, 24)].

The TCR affinity for the oligomers is generally taken to be the free oligomer concentration when the amount of bound oligomers is half of the plateau or maximal level ($K_{D,olig}$). The ratio between $K_{D,olig}$ and the equilibrium constant (K_D) for monovalent binding of the same TCR to the same pMHC as monomer ($K_{D,olig}/K_D$, called the enhancement factor) was previously seen to be more pronounced for low-affinity than high-affinity TCR–pMHC interactions (19). It was thus not surprising that for m33, the very high-affinity TCR (19), the oligomer concentration that resulted in half-maximal binding was about the same with CD8^{pos} and CD8^{neg} hybridomas (Fig. 1*B*). However, for the much lower affinity wild-

type 2C TCR, the half-maximal concentrations with $CD8^{neg}$ and $CD8^{pos}$ hybridomas, 2.8 nM and 4.8 nM, respectively, were surprisingly also similar (Fig. 1*B*); the small difference implied that the coexpressed CD8 had, if anything, a negative effect on this TCR's affinity for pMHC. Among the questions raised by these findings is whether the SA-oligomers can engage all cell-surface TCR and measure TCR affinity for pMHC.

Do oligomers at high concentration saturate cell-surface TCRs?

To determine if saturation is approached, we measured the number of surface TCR molecules per cell, using fluorescein-labeled mAbs to various TCR domains (Cβ and Vβ8) and to the TCR-associated protein, CD3; we also used the fluorescein-labeled clonotypic Ab 1B2, which is specific for the 2C TCR (but does not bind to the 2C mutant m33). The results are shown in Fig. 2*A*, 2*B*, and summarized in Table I. As noted in the legend to Table I, the number of surface TCR molecules per cell was estimated to be twice the number of Ab molecules bound (to account for Ab binding bivalently). The number of TCR may be slightly lower, as some anti-TCR Ab molecules may be bound monovalently. Studies have shown that although the TCR complex can assemble as a monomer (36), the TCR may exist on the cell surface, at least in part, as a dimer (37–39) or oligomer (40, 41) and may preferentially bind Abs bivalently (39). It is, of course, possible that not all the TCRs measured by Ab quantification are conformationally able to bind pMHC at any given time.

As the oligomers are trimeric on average (Fig. 1*A*), and are thought to behave functionally as trimers, the number of TCR engaged by bound oligomers was taken to be (at most) three times the maximum number of bound oligomers in the titrations shown in Fig. 1*B*, 1*C*. From the ratio of oligomer-engaged TCR to the total number of TCR it appeared that not >10–30% of cell surface TCR was maximally engaged by bound oligomers.

Dissociation kinetics of cell-bound tetramers

One possible reason for the apparent failure to engage more cell surface TCR is that bound oligomers are lost when cells are washed prior to flow cytometry. To evaluate this possibility, we examined the dissociation of SIY/K^b oligomers from oligomer-stained cells (Fig. 3*A*, 3*B*). The steps involved in dissociation can be represented by:

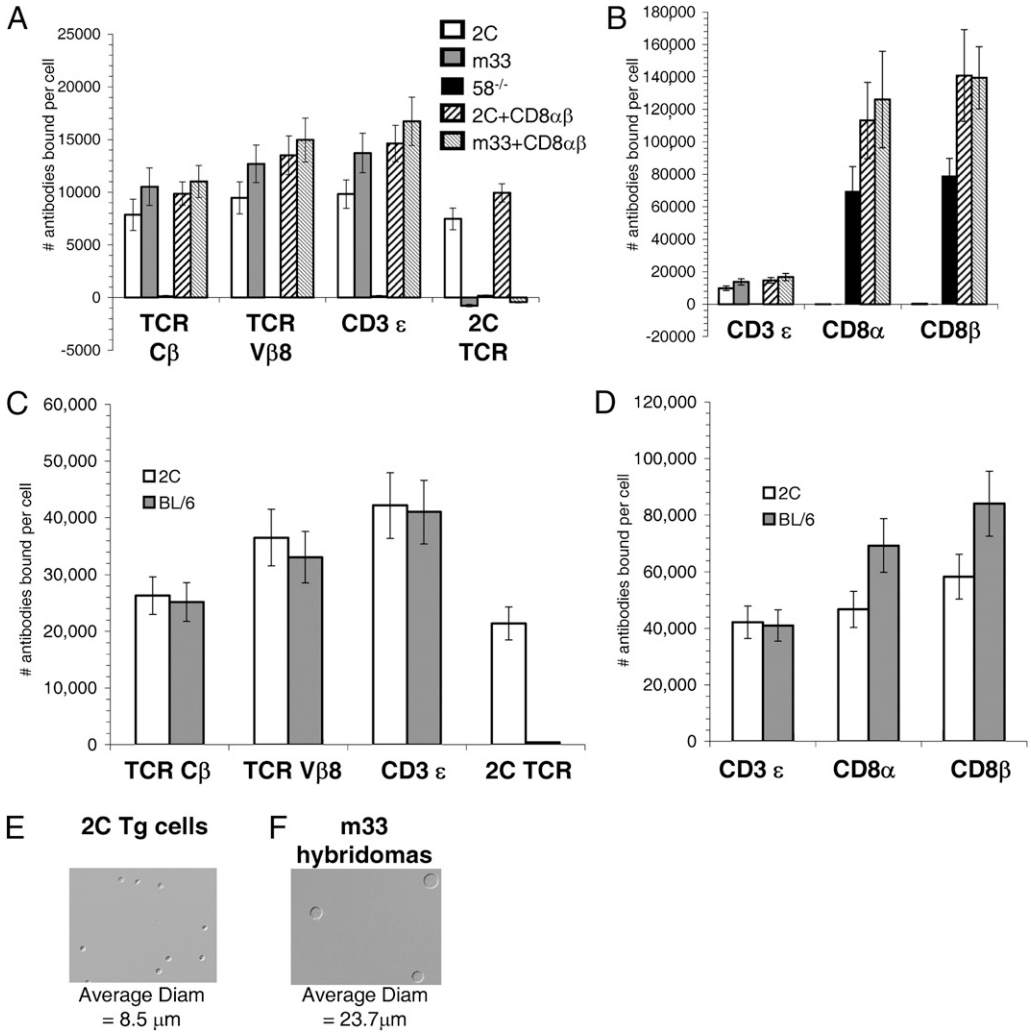

FIGURE 2. Detection of T cell receptor and CD8 epitopes on T cell hybridomas and transgenics. Quantification of molecules per cell is derived from flow cytometry staining data using calibrated, fluorescein-labeled Abs and comparing to two independent batches of fluorescein-labeled beads. *A–D*, Staining of cell-surface epitopes including (*A, C*) TCR Cβ (clone H57-597), TCR Vβ8 (clone F23.1), CD3ε (clone 145-2C11), the 2C TCR specifically (clone 1B2), and (*B, D*) CD8α (clone 53-6.7) and CD8β (clone 53-5.8) on (*A, B*) T cell hybridomas or (*C, D*) mouse T cells. Error bars represent the SD for at least two and up to eight repetitions for each individual measurement. *E* and *F*, Contrast images showing the size differences between (*E*) mouse T cells (2C TCR transgenic) and (*F*) T cell hybridomas (m33 TCR).

Table I. Cell surface density of TCR and CD8 on splenic T cells and transduced T cell hybridomas

T Cells	Average No. Ab Molecules Bound per Cell ($\times 10^3$) Abs to: TCR Cβ[a]	TCR Vβ8[b]	CD3ε[c]	2C TCR (Clonotype)[d]	CD8α[e]	CD8β[f]	Average No. TCR per cell[g] ($\times 10^3$)
T cell hybridomas expressing							
CD8αβ only	0.2	0.1	0.2	0.2	57.4	78.9	0
2C TCR	6.8	8.7	9.8	7.5	−0.1	0.2	15.3
2C TCR + CD8αβ	9.7	13.5	15.4	6.3	85.8	117	19.7
m33 TCR	9.3	12.4	13.7	−0.8	−0.01	−0.03	21.7
m33 TCR + CD8αβ	11.0	14.5	16.7	−0.4	102	140	25.5
$CD8^+$ splenic T cells							
C57BL/6	25.6	33.0	41.0	0.4	69.3	84.0	58.2
2C TCR transgenic	26.7	36.5	42.2	21.4	46.7	58.3	56.4

[a]H57-597 Ab (BD Pharmingen).
[b]F23.1 Ab (BD Pharmingen).
[c]145-2C11 Ab (BD Pharmingen).
[d]1B2 Ab labeled with FITC.
[e]53-6.7 Ab (BD Pharmingen).
[f]53-5.8 Ab (BD Pharmingen).
[g]Estimated maximum number of TCR per cell line taken as twice the average of TCR Cβ, TCR Vβ8, and 2C TCR (for 2C TCR transgenic or transduced T cells).

$$L \equiv T \underset{\mu}{\overset{3k_{off}}{\rightleftharpoons}} L = T \underset{2\mu}{\overset{2k_{off}}{\rightleftharpoons}} L - T \xrightarrow{k_{off}} L_{sol}, \qquad (1)$$

where T refers to available TCR sites on the cell surface, $L \equiv T$ is the number of oligomers bound by three pMHC complexes, $L = T$ is the number bound by two pMHCs, and L-T is the number bound by one pMHC, Dissociation of L-T loses oligomers into solution (L_{sol}). The off-rate constants for dissociation (k_{off}) are considered to be the same as measured by SPR with monomeric pMHC except for the statistical factors shown in Eq. 1. However, the on-rates will differ by more than these statistical factors. When a TCR monomer binds to immobilized pMHC complexes (as in an SPR experiment), it gives up the entropic freedom of sampling a multitude of configurations in solution and orients itself in the correct configuration. This entropic penalty is contained in the free energy barrier that is included in the measured value of the on-rate constant (k_{on}). The same entropic factors (with minor differences due to potential steric constraints) are also relevant when the first pMHC of an oligomer binds, but after one of an oligomer's pMHC binds to a cell, the binding rate of the other pMHC of that oligomer is determined by rather different entropic changes. Therefore, the effective on-rate for the binding of the second and third pMHC, designated μ, will differ from that obtained from SPR measurements with monomeric pMHC by more than statistical factors. By assuming that interconversion among bound states of the oligomer (single, double, or triple-bonded) is relatively rapid, it can be shown (see Appendix A: Model Equations) that

$$\frac{L_{bound,t}}{L_{bound,0}} = \exp[-k_{off}^{eff} t] = \exp\left[-\frac{k_{off}^3}{3k_{off}^2 + 3k_{off}\mu + \mu^2} t\right] \approx \exp\left[-\frac{k_{off}^3}{\mu^2} t\right], \qquad (2)$$

where $L_{bound,t}$ is the amount of bound oligomer at a particular time (t), and $L_{bound,0}$ is the amount bound initially.

As seen in Fig. 3*A*, 3*B*, the dissociation rates from each of the hybridomas and T cells could indeed be fitted by a single-value exponential decay constant (k_{off}^{eff}), which is equivalent to $k_{off}^3/(3k_{off}^2 + 3k_{off}\mu + \mu^2)$ in Eq. 2. This suggests that we are in a regimen where the assumption of a rapid interconversion of bound states is valid, as has been assumed previously (32).

From the experimentally determined k_{off}^{eff} values (Fig. 3), the amounts of oligomer lost during the ~8 min spent in washing oligomer-stained cells (see *Materials and Methods*) can be estimated. Correction for these losses still indicated that saturation was far from having been achieved before washing cells, especially for the freshly isolated $CD8^{pos}$ splenic T cells. These corrections were based initially on dissociation rates measured at 25°C (Fig. 3*A*, 3*B*). But, as the cells were washed in the cold (~10°C), where longer $t_{1/2}$ values are expected, the actual losses were likely even smaller. To find out how much smaller, we took advantage of the intrinsic (monovalent) on- and off-rates for the binding of the SIY/K^b complex by the 2C and m33 TCR measured by SPR at 25°C and 10°C (Ref. 19 and Table III). Based upon the following argument, these intrinsic rates could be used, together with the k_{off}^{eff} measured at 25°C, to estimate k_{off}^{eff} at 10°C.

As is discussed in Appendix A: Model Equations, the difference in dimensions of μ (measured in s^{-1}) and intrinsic monovalent on-rates, k_{on} (which are measured for reactants in solution and expressed in $M^{-1}s^{-1}$) arises because μ already incorporates the TCR concentration in the form of the cell-surface density in the vicinity of the bound oligomer; i.e., $\mu = k_{on} \times$ local surface density of TCR, where k_{on} is essentially the monovalent k_{on} as measured by SPR (see below). On the assumption that the local and overall cell-surface TCR density for a given T cell is the same at 25°C and 10°C, it follows that

$$\mu_{10°C} = \mu_{25°C} \frac{k_{on,10°C}}{k_{on,25°C}}. \qquad (3)$$

Values for k_{on} at the two temperatures are shown in Table III for m33 and several other engineered mutants of the 2C TCR. From these values, k_{off}^{eff} at 10°C can be obtained by using the relationships outlined in the mathematical model. The correction for losses during an 8 min wash at ~10°C indicate that before oligomer-stained cells were washed only ~15% of the TCR molecules on splenic $CD8^{pos}$ T cells and ~40% of those on the T cell hybridomas were engaged by the SA-oligomers at the highest oligomer concentrations tested (Fig. 1*B*, 1*C*, Table II).

The extent to which bound oligomers are lost by dissociation from stained cells varies with the decay constant ($k_{off,app}$) and the time spent preparing cells for flow cytometry (Fig. 3*C*). Because k_{off}^{eff} and intrinsic TCR–pMHC affinity (K_D) are correlated (Table III) (12, 16, 18, 19, 26), these losses are negligible for the engi-

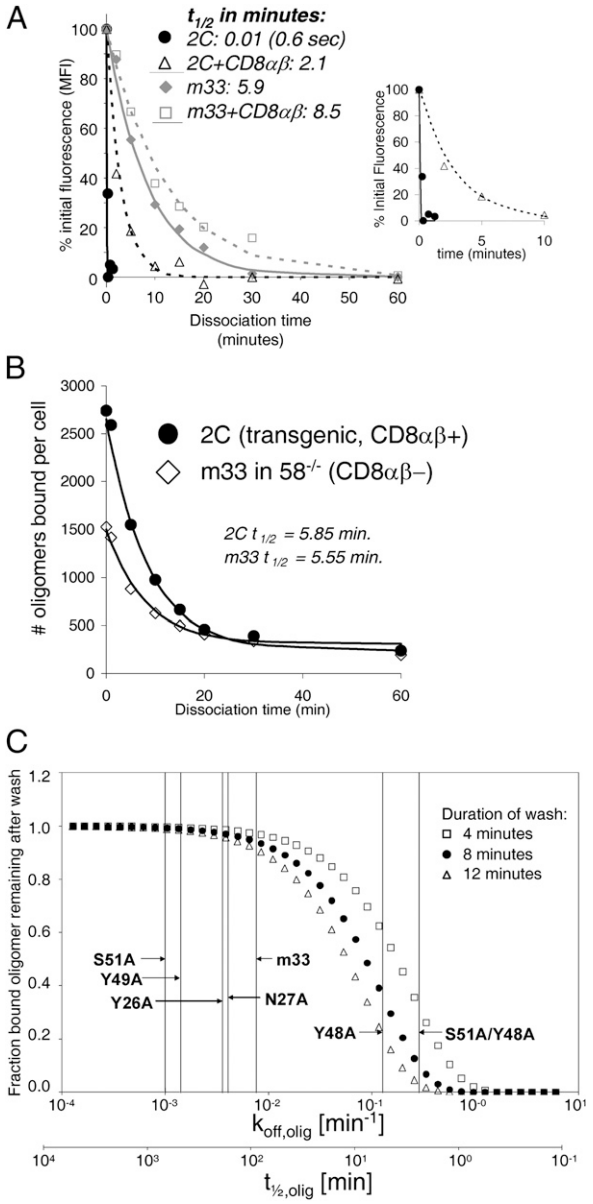

FIGURE 3. MHC oligomer dissociation from T cells. *A* and *B*, Remaining associated fluorescent pMHC oligomer measurements were made for (*A*) 2C hybridomas with (open triangles) or without (closed circles) CD8 (highlighted in *inset*), and m33 with (open squares) or without (closed diamonds) CD8. *B*, 2C TCR transgenic T cells (closed circles) and m33 hybridomas ($CD8^-$, open diamonds). Dissociation data for *A* and *B* were fit by the equation describing a first-order exponential decay. *C*, Simulated effect of dissociation of bound oligomers on washing the cells over a 4, 8, or 12 min period in the cold (4°–10°C) prior to flow cytometry, showing the effect of $k_{off,app}$ on the level of persisting oligomers. Vertical bars indicate approximate $k_{off,app}$ values calculated for different 2C receptor mutants.

neered high affinity TCR. But for lower affinity TCR, such as the 2C TCR with the Y48 or S51/Y48 mutations, ~80–90% of bound oligomers would be lost under conditions that are commonly used to prepare oligomer-stained cells for flow cytometry.

CD8 effect on TCR–pMHC binding

From Fig. 3, it is evident that the presence of CD8αβ on the cells led to slower oligomer dissociation. For the wild-type 2C TCR on the $CD8^{neg}$ hybridoma, dissociation was so fast that the rate could hardly be measured. However, with $CD8^{pos}$ hybridoma that expressed the same TCR at about the same level, $t_{1/2,app}$ increased to >2 min (Fig. 3*A* and *inset*). For hybridomas that expressed the high-affinity m33 TCR, the oligomer dissociation $t_{1/2}$ increased from 5.9 min on $CD8^{neg}$ cells to 8.5 min on $CD8^{pos}$ cells (Fig. 3*B*). To compare T cell hybridomas with T cells freshly isolated from mice, $CD8^{pos}$ T cells from $Rag^{-/-}$ 2C TCR transgenic splenocytes were examined side-by-side with $CD8^{neg}$ m33 TCR^+ hybridomas (Fig. 3*B*). Interestingly, the oligomer off-rate was nearly identical for the two cell types, despite marked differences in TCR affinities, TCR densities, and CD8 expression.

Why do oligomers dissociate more slowly from $CD8^{pos}$ 2C T cells than from $CD8^{pos}$ hybridomas that express the same TCR ($t_{1/2,app}$ = 5.85 and 2.1 min, respectively) (Fig. 3*A*, 3*B*)? The answer likely lies in the much greater number of TCR per cell on the $CD8^{pos}$ T cells (~56,000/cell on the $CD8^{pos}$ T cells versus ~25,000/cell on the $CD8^{pos}$ hybridoma cells, Fig. 2*C*, 2*D*, Table I). Moreover, the splenic $CD8^{pos}$ T cell diameter is about one-third that of hybridomas (Fig. 2*E*, 2*F*). These differences mean that the cell-surface TCR density is on average ~20-fold greater on the splenic T cells than on the hybridomas (188/μm^2 versus 8/μm^2), resulting in the larger multivalent on-rate (μ) and smaller k_{off}^{eff} (larger $t_{1/2,app}$) on the T cells. This average density found on normal and transgenic T cells is consistent with what has been observed previously (42). Precise measurements of density are difficult, however, as the membranes of lymphocytes are not simple spheres (43), and local variations in TCR density are expected (reviewed in Ref. 44), which could influence binding properties. Because the intrinsic k_{off} rate is expected to be the same from the 2C TCR, whether expressed by splenic T cells or the transduced hybridomas, the greater stability of the SA-oligomers on the splenic T cells can be attributed to the faster on-rate (μ) on the T cells.

Oligomer equilibrium binding constants ($K_{D,olig}$)

Although cell-bound pMHC oligomers do not saturate cognate cell-surface TCR, the titration curves in Fig. 1*B*, 1*C* indicate that they saturate a subset of these TCR (19). For this subset, the processes that occur on oligomer binding at steady state can be represented as:

$$L_{sol} + T \underset{k_{off}}{\overset{k'_{on}}{\rightleftharpoons}} L - T \underset{2k_{off}}{\overset{2\mu}{\rightleftharpoons}} L = T \underset{3k_{off}}{\overset{\mu}{\rightleftharpoons}} L \equiv T, \qquad (4)$$

where all of the terms are defined as in Eq. 1 except for k'_{on}, which refers to the on-rate for the first pMHC of the oligomer to bind. We take k'_{on} to be the monomeric pMHC–TCR on-rate (measured for example by SPR), except for a statistical factor that takes into account the number of pMHC per oligomer (three in the present case). The binding data can be treated according to the Langmuir adsorption isotherm to obtain an expression for the fraction of cell-surface sites (i.e., TCR) occupied by the pMHC oligomers as a function of the free oligomer concentration. Accordingly,

$$\frac{\theta}{1-\theta} = \left[\frac{k'_{on}\, L_{sol}(3k_{off}^{\,2} + 3k_{off}\mu + \mu^2)}{k_{off}^{\,3}}\right] = \frac{k'_{on} L_{sol}}{k_{off}^{eff}}, \qquad (5)$$

where L_{sol} is the concentration of oligomers in solution, and θ is the fraction of sites occupied by oligomers (singly, doubly, or triply bound). In deriving Eq. 5 (see Appendix A: Model Equations), we have assumed that the concentration of oligomers in solution is essentially equal to the initial oligomer concentration and that this approximation is valid when the latter quantity is relatively large.

Table II. Extent of TCR occupancy by SA-linked MHC oligomers

T Cells	Total No. TCR per cell[a]	Maximum No. TCR Engaged by pMHC Oligomers[b]	Maximum No. TCR Engaged/Total No. TCR		
			Measured	Corrected for Losses during 8 Min Wash at: 25°C[c]	10°C[d]
T cell hybridomas expressing					
2C TCR	15,300	2985	0.20	—	—
2C TCR and CD8αβ	19,700	2058	0.10	—	0.22[e]
m33 TCR	21,700	6225	0.29	0.73	0.37
m33 TCR and CD8αβ	25,500	6309	0.25	0.48	0.30
$CD8^+$ splenic T cells					
C57BL/6	58,200	(450)	—	—	—
2C TCR transgenic	56,400	7050	0.13	0.32	0.13[e]

[a]From Table I.
[b]Maximum level of MHC oligomer saturation measured, allowing for three MHC engaged per SA-oligomer.
[c]Maximum TCR occupancy estimated at steady-state correcting for losses during a preanalysis wash carried out at 25°C.
[d]Maximum TCR occupancy estimated at steady-state correcting for losses during a preanalysis wash carried out at 10°C.
[e]Conversion of $k_{off,olig}$ for 2C uses k_{on} and k_{off} for 2C measured at 25°C, but k_{on} and k_{off} for the closely-related TCR Y48 measured at 10°C (Table III).

From the titration shown in Fig. 1*C*, the apparent affinity ($K_{D,olig}$) of the 2C TCR on splenic $CD8^{pos}$ T cells for SA-SIY/K^b oligomers is ~1 nM, as determined by the free oligomer concentration at 50% maximum bound. Comparisons of $K_{D,olig}$ to monovalent K_D are useful to demonstrate the benefits of multivalent ligand binding to TCR (e.g., the $K_D/K_{D,olig}$ ratio has been termed an enhancement factor) (19, 45).

Discussion

This study confirms previous indications that SA-based pMHC oligomers (tetramers) bind stably to only a fraction of cognate cell surface TCR (19). The fraction amounted to ~15% of the TCR on $CD8^{pos}$ splenic T cells from 2C TCR transgenic mice and ~40% on a TCR-transduced hybridoma line. These less-than-saturating levels arise in part from losses of bound oligomers when oligomer-stained cells are washed. The extent of these losses depends on the dissociation or decay constant, k_{off}^{eff}, which is related to TCR–pMHC affinity (Fig. 3*C* and Eq. 2). For T cells for which TCR binds oligomers weakly (large k_{off}^{eff}), nearly all bound oligomers may be lost by dissociation when cells are subjected to commonplace washing conditions. This effect could account for reports of tetramer-negative functionally competent $CD8^{pos}$ T cells (9–12). Losses of bound oligomers by dissociation from low-affinity TCR may also well account for the recent report of a surprisingly high frequency of $CD4^{pos}$ T cells that respond specifically to pMHC but are not stained by the corresponding tetramers (13). The frequency of such tetramer-negative, functionally competent T cells would be expected to be higher in $CD4^{pos}$ than in $CD8^{pos}$ T cell populations because of differences in their coreceptor ectodomain binding to MHC; CD8 generally binds weakly to class I MHC but CD4 binds hardly at all to class II MHC (46, 47).

It is likely that the oligomers bind stably (multivalently) only to those TCR molecules that are closely clustered. The spacing between biotin (pMHC) binding sites on SA is 2–4 nm (48), whereas TCR, if uniformly distributed on the cell surface, would generally be much further apart (separated on average by ~60–70 nm on a T cell of 8.5 μm diameter with 56,000 TCR molecules per cell [Fig. 2*E*, Table I]). But cell-surface TCR, like many other integral membrane proteins, are aggregated into groups ("islands"), some depending upon cholesterol (lipid rafts) for their clustering (15, 49–51; reviewed in Ref. 52). Whether the SA-oligomers bind selectively to particular TCR clusters is not clear. The stronger binding of pMHC dimers to activated than to naive T cells and abolition of this difference by reducing cholesterol content of the cell membranes (15) indicate that oligomer binding has the potential to be developed into a useful procedure to define the size and character of TCR clusters on cells that differ functionally or in developmental status.

For the TCR subset that can stably engage SA-oligomers, an apparent equilibrium constant for the oligomer–TCR interaction ($K_{D,olig}$) can be defined as the free SA-oligomer concentration that

Table III. Binding of SIY/K^b monomer by various TCR measured by SPR at different temperatures

TCR	10°C[a]				25°C[b]			
	k_{on} ($M^{-1}s^{-1}$)	k_{off} (s^{-1})	K_D (nM)	$k_{off,olig}$ (min^{-1})[c]	k_{on} ($M^{-1}s^{-1}$)	k_{off} (s^{-1})	K_D (nM)	$k_{off,olig}$ (min^{-1})
m33	2.5×10^5	0.0036	17.1	0.008	13.7×10^5	0.015	16	0.08
S51	3.5×10^5	0.0013	3.97	0.001	5.15×10^5	0.008	15	0.05
Y26	3.3×10^5	0.0023	7.2	0.004	8.5×10^5	0.013	17	0.12
Y49	2.3×10^5	0.0019	8.6	0.001	2.8×10^5	0.012	47	0.07
N27	2.8×10^5	0.0036	12.7	0.004	5.2×10^5	0.021	40	0.19
S51/Y48	1.7×10^5	0.051	305	0.29	1.36×10^5	0.076	540	1.49
Y48	1.65×10^5	0.185	1130	0.12	1.36×10^5	0.35	2900	3.20

[a]Measurements of monovalent binding properties carried out at 10°C by SPR.
[b]Values for binding of SIY/K^b at 25°C reprinted with permission from Chervin et al. (19).
[c]$k_{off,olig}$ at 10°C estimated from monovalent binding properties and from $k_{off,olig}$ values at 25°C, using Eq. (2) and the relationship: $\mu_{10°C} = \mu_{25°C} \times k_{on,10°C}/k_{on,25°C}$.

Table IV. Equilibrium constants (K_D) for 2C TCR binding the SIY/K^b (pMHC) complex measured under various conditions

Assay Conditions	K_D (μM)	Reference
Soluble, recombinant 2C TCR and SIY/K^b	32	23
SPR	27	24
	36	19
Soluble monomeric SIY/K^b	0.1	54
Inhibition of [^{125}I]-Fab 1B2 binding to $CD8^+$ T cells	0.33	53
Dimeric SIY/K^b-IgG binding to		
Naive 2C transgenic T cells	0.004 (4°C)	15
	0.077 (37°C)	15
Activated 2C transgenic T cells	0.001 (4°C)	15
	0.064 (37°C)	15
Streptavidin-oligomers of SIY/K^b binding to		
$CD8^-$ 2C T cell hybridomas	0.011	19
	0.0041	[a]
$CD8^+$ 2C T cell hybridomas	0.0023	[a]
$CD8^-$ m33 T cell hybridomas	0.0010	[a]
$CD8^+$ m33 T cell hybridomas	0.0016	[a]
$CD8^+$ 2C transgenic splenic T cells	0.0016	[a]

Measurements at 25°C unless otherwise indicated.
[a]Values measured in current work.

leads to half-saturation of that TCR subset (Eq. 5), the main uncertainty being the maximum level. From the titration shown in Fig. 1*C*, $K_{D,olig}$ is ~1 nM for the 2C TCR–SIY/K^b oligomer interaction on $CD8^{pos}$ T cells. This value is compared in Table IV with others measured for the same TCR (2C) and the same Ag (SIY/K^b complex) under different conditions. The values range from ~30 μM (in the micromolar range commonly found by SPR for many rTCR and pMHC pairs) to a 300-fold higher affinity for the binding of soluble SIY/K^b monomer to the 2C TCR and CD8 on intact $CD8^{pos}$ T cells and the much higher values found with Ig-based dimers and SA-oligomers on $CD8^{pos}$ T cells. Although the presumably clustered TCR molecules that bind SA-oligomers stably (multivalently) constitute a small fraction of all cell surface TCR (41), they and nonclustered TCR have the same intrinsic (monovalent) affinity. This uniformity is indicated by the linearity of Scatchard plots (1, 15) and by the Sips distribution (53).

The binding of pMHC oligomers to cell-surface TCR approximates more closely than the other conditions in Table IV to the quasi 2D interactions that occur under physiological conditions at the interface of T cells and target cells or other APCs. Recent studies have reported the kinetics of such 2D interactions to be exceptionally fast and their apparent affinities much higher than for the same interactions under three-dimensional conditions (2, 3).

Finally, it is worth commenting on the contribution of CD8αβ in the trimolecular CD8–pMHC–TCR reaction. Experimental findings (32) and computational analysis (46) concur in showing that the CD8 ectodomain's binding to the MHC α3 domain increases the lifetime of the TCR–pMHC bond only modestly, 2-fold at most. For SA-linked oligomers, which are effectively trimeric, the CD8 effect can be increased up to 8-fold because k_{off}^{eff} is proportional to $(k_{off})^3$ (Eq. 2 and Refs. 32, 46). The CD8 effect on hybridomas that expressed the high-affinity TCR (m33) is consistent with these values: $t_{1/2}$ is ~1.4-fold greater for the $CD8^{pos}$ than $CD8^{neg}$ cells (Fig. 3*A*). However, for hybridomas that express the lower affinity 2C TCR, $t_{1/2}$ is 20-fold greater for the $CD8^{pos}$ than the $CD8^{neg}$ cells, which exceeds the estimated upper limit of eight and reflects the greater dissociative losses of bound oligomers from relatively low-affinity TCR (Fig. 3*C*). The still far greater difference, ~50-fold, between the $CD8^{neg}$ hybridoma and $CD8^{pos}$ splenic T cells that express the same TCR (2C) ($t_{1/2}$ ~0.1 min versus 5.85 min), likely arises from the additional effect of the ~20-fold greater surface density of the TCR on the splenic T cells, resulting in an increase in the multivalent on-rate (μ) and from the proportionality of k_{off}^{eff} to $\frac{k_{off}{}^3}{\mu^2}$ (Eq. 2).

Appendix A: Model Equations

Dissociation of bound oligomers

$$L \equiv T \underset{\mu}{\overset{3k_{off}}{\rightleftharpoons}} L = T \underset{2\mu}{\overset{2k_{off}}{\rightleftharpoons}} L - T \xrightarrow{k_{off}} L_{sol}, \quad \text{(Scheme 1)}$$

where T refers to available TCR sites on the cell surface, $L \equiv T$ is the number of oligomers bound by three pMHC complexes, $L = T$ is the number bound by two pMHCs, and L-T is the number bound by one pMHC, dissociation of L-T loses oligomers into solution (L_{sol}).

We assume that for each pMHC–TCR interaction, k_{off} and μ (the multivalent on rate, see text) are independent of the binding of neighboring MHC with TCR. Thus, stoichiometric coefficients in front of k_{off} and μ correspond to the number of pMHCs available for binding/unbinding.

The following differential equations were used to describe interconversion among bound forms and loss of bound forms in accord with Scheme (1):

$$\frac{d[L-T]}{dt} = -k_{off}[L-T] + 2k_{off}[L=T] - 2\mu[L-T], \quad \text{(A1)}$$

$$\frac{d[L=T]}{dt} = -2k_{off}[L=T] - \mu[L=T] + 2\mu[L-T] + 3k_{off}[L\equiv T], \quad \text{(A2)}$$

and

$$\frac{d[L\equiv T]}{dt} = -3k_{off}[L\equiv T] + \mu[L=T]. \quad \text{(A3)}$$

Derivation of text Eq. 2 and 5

Text Eq. 2. Concentration of oligomers (L) bound to cell-surface TCR (T) is equal to the sum of all bound forms:

$$L_B = L - T + L = T + L \equiv T. \quad \text{(A4)}$$

Loss of bound oligomers is determined by dissociation of the singly bound form:

$$\frac{dL_B}{dt} = -k_{off}^{eff} L_B = -k_{off}[L-T]. \quad \text{(A5)}$$

As our oligomer dissociation data exhibit exponential decay kinetics, we can safely assume a rapid equilibrium and interconvertibility (mass equilibrium) of bound forms, as has been assumed previously (32). Applying this assumption, we get:

$$[L=T] = \frac{\mu}{k_{off}}[L-T], \text{and} \quad \text{(A6)}$$

$$[L \equiv T] = \frac{\mu}{3k_{off}}[L=T] = \frac{\mu^2}{3k_{off}^2}[L-T]. \quad \text{(A7)}$$

Plugging in (A6-7) to (A4):

$$L_B = [L-T]\left(1 + \frac{\mu}{k_{off}} + \frac{\mu^2}{3k_{off}^2}\right) = [L-T]\left(\frac{3k_{off}^2 + 3k_{off}\mu + \mu^2}{k_{off}^2}\right). \quad \text{(A8)}$$

Plugging (A8) in to (A5) yields Text Eq. 2:

$$\frac{L_{bound,t}}{L_{bound,0}} = \exp[-k_{off}^{eff} t] = \exp\left[-\frac{k_{off}^3}{3k_{off}^2 + 3k_{off}\mu + \mu^2} t\right] \approx \exp\left[-\frac{k_{off}^3}{\mu^2} t\right],$$

where the approximate equality can be applied under the conditions where $\mu >> k_{off}$, as is true for all of the interactions described in this study. Where $\mu \leq k_{off}$, the roots of the quadratic equation for μ can be solved.

Derivation of Text Eq. 5

At equilibrium, the rate of oligomer association is equal to the rate of oligomer dissociation:

$$k_{on}^{'} T_{free} \cdot L_{sol} = k_{off}^{eff} L_{bound},$$

where k'_{on} is on-rate (k_{on}) for the monomeric pMHC–TCR interaction, as measured for instance by SPR, modified by the number of pMHC per streptavidin molecule.

If θ is taken to be the fraction of occupied receptors, $T_{free} = (1-\theta)T_{total}$ and $L_{bound} = \theta T_{total}$, Eq. 5 from the main text then follows:

$$\frac{\theta}{1-\theta} = \left[\frac{k_{on}^{'} L_{sol}(3k_{off}^2 + 3k_{off}\mu + \mu^2)}{k_{off}^3}\right] = \frac{k_{on}^{'} L_{sol}}{k_{off}^{eff}}.$$

Eq. 5 resembles the Scatchard equation. That equation, arguably the most widely used one in immunology, was originally developed (30) to account for the equilbrium binding of small molecules and ions to proteins. For ligand–protein interactions, it is usually expressed as $r/(n-r) = Kc$, where r represents moles bound ligand, n the moles of ligand maximally bound, c the free ligand concentration, and K the equilibrium (association) constant. Independent derivations of Scatchard's equation have generally been based upon the distribution of bound and free ligands at equilibrium (29, 31). In contrast, Eq. 5 above was derived from the kinetics of multivalent ligand binding to cell surface receptors. If, however, Eq. 5 were applied to monovalent ligand–receptor interactions, μ would become zero, k_{on}' would correspond to the intrinsic association rate, k_{on}, and Eq. 5 would then be equivalent to the Scatchard equation.

Acknowledgments

We thank the staff of the University of Illinois Carver Biotechnology Center for assistance with flow cytometry and SPR studies.

Disclosures

The authors have no financial conflicts of interest.

References

1. Sykulev, Y., A. Brunmark, T. J. Tsomides, S. Kageyama, M. Jackson, P. A. Peterson, and H. N. Eisen. 1994. High-affinity reactions between antigen-specific T-cell receptors and peptides associated with allogeneic and syngeneic major histocompatibility complex class I proteins. *Proc. Natl. Acad. Sci. USA* 91: 11487–11491.
2. Huang, J., V. I. Zarnitsyna, B. Liu, L. J. Edwards, N. Jiang, B. D. Evavold, and C. Zhu. 2010. The kinetics of two-dimensional TCR and pMHC interactions determine T-cell responsiveness. *Nature* 464: 932–936.
3. Huppa, J. B., M. Axmann, M. A. Mörtelmaier, B. F. Lillemeier, E. W. Newell, M. Brameshuber, L. O. Klein, G. J. Schütz, and M. M. Davis. 2010. TCR-peptide-MHC interactions in situ show accelerated kinetics and increased affinity. *Nature* 463: 963–967.
4. Dal Porto, J., T. E. Johansen, B. Catipović, D. J. Parfiit, D. Tuveson, U. Gether, S. Kozlowski, D. T. Fearon, and J. P. Schneck. 1993. A soluble divalent class I major histocompatibility complex molecule inhibits alloreactive T cells at nanomolar concentrations. *Proc. Natl. Acad. Sci. USA* 90: 6671–6675.
5. Serbina, N., and E. G. Pamer. 2003. Quantitative studies of CD8+ T-cell responses during microbial infection. *Curr. Opin. Immunol.* 15: 436–442.
6. Vollers, S. S., and L. J. Stern. 2008. Class II major histocompatibility complex tetramer staining: progress, problems, and prospects. *Immunology* 123: 305–313.
7. Xu, X. N., and G. R. Screaton. 2002. MHC/peptide tetramer-based studies of T cell function. *J. Immunol. Methods* 268: 21–28.
8. Altman, J. D., P. A. Moss, P. J. Goulder, D. H. Barouch, M. G. McHeyzer-Williams, J. I. Bell, A. J. McMichael, and M. M. Davis. 1996. Phenotypic analysis of antigen-specific T lymphocytes. *Science* 274: 94–96.
9. Burrows, S. R., N. Kienzle, A. Winterhalter, M. Bharadwaj, J. D. Altman, and A. Brooks. 2000. Peptide-MHC class I tetrameric complexes display exquisite ligand specificity. *J. Immunol.* 165: 6229–6234.
10. Buslepp, J., R. Zhao, D. Donnini, D. Loftus, M. Saad, E. Appella, and E. J. Collins. 2001. T cell activity correlates with oligomeric peptide-major histocompatibility complex binding on T cell surface. *J. Biol. Chem.* 276: 47320–47328.
11. Hernández, J., P. P. Lee, M. M. Davis, and L. A. Sherman. 2000. The use of HLA A2.1/p53 peptide tetramers to visualize the impact of self tolerance on the TCR repertoire. *J. Immunol.* 164: 596–602.
12. Laugel, B., H. A. van den Berg, E. Gostick, D. K. Cole, L. Wooldridge, J. Boulter, A. Milicic, D. A. Price, and A. K. Sewell. 2007. Different T cell receptor affinity thresholds and CD8 coreceptor dependence govern cytotoxic T lymphocyte activation and tetramer binding properties. *J. Biol. Chem.* 282: 23799–23810.
13. Sabatino, J. J., Jr., J. Huang, C. Zhu, and B. D. Evavold. 2011. High prevalence of low affinity peptide-MHC II tetramer-negative effectors during polyclonal CD4+ T cell responses. *J. Exp. Med.* 208: 81–90.
14. Busch, D. H., and E. G. Pamer. 1999. T cell affinity maturation by selective expansion during infection. *J. Exp. Med.* 189: 701–710.
15. Fahmy, T. M., J. G. Bieler, M. Edidin, and J. P. Schneck. 2001. Increased TCR avidity after T cell activation: a mechanism for sensing low-density antigen. *Immunity* 14: 135–143.
16. Holmberg, K., S. Mariathasan, T. Ohteki, P. S. Ohashi, and N. R. Gascoigne. 2003. TCR binding kinetics measured with MHC class I tetramers reveal a positive selecting peptide with relatively high affinity for TCR. *J. Immunol.* 171: 2427–2434.
17. Slifka, M. K., and J. L. Whitton. 2001. Functional avidity maturation of CD8(+) T cells without selection of higher affinity TCR. *Nat. Immunol.* 2: 711–717.
18. Crawford, F., H. Kozono, J. White, P. Marrack, and J. Kappler. 1998. Detection of antigen-specific T cells with multivalent soluble class II MHC covalent peptide complexes. *Immunity* 8: 675–682.
19. Chervin, A. S., J. D. Stone, P. D. Holler, A. Bai, J. Chen, H. N. Eisen, and D. M. Kranz. 2009. The impact of TCR-binding properties and antigen presentation format on T cell responsiveness. *J. Immunol.* 183: 1166–1178.
20. Udaka, K., K. H. Wiesmüller, S. Kienle, G. Jung, and P. Walden. 1996. Self-MHC-restricted peptides recognized by an alloreactive T lymphocyte clone. *J. Immunol.* 157: 670–678.
21. Holler, P. D., L. K. Chlewicki, and D. M. Kranz. 2003. TCRs with high affinity for foreign pMHC show self-reactivity. *Nat. Immunol.* 4: 55–62.
22. Shusta, E. V., P. D. Holler, M. C. Kieke, D. M. Kranz, and K. D. Wittrup. 2000. Directed evolution of a stable scaffold for T-cell receptor engineering. *Nat. Biotechnol.* 18: 754–759.

23. Garcia, K. C., M. D. Tallquist, L. R. Pease, A. Brunmark, C. A. Scott, M. Degano, E. A. Stura, P. A. Peterson, I. A. Wilson, and L. Teyton. 1997. Alphabeta T cell receptor interactions with syngeneic and allogeneic ligands: affinity measurements and crystallization. *Proc. Natl. Acad. Sci. USA* 94: 13838–13843.
24. Jones, L. L., L. A. Colf, J. D. Stone, K. C. Garcia, and D. M. Kranz. 2008. Distinct CDR3 conformations in TCRs determine the level of cross-reactivity for diverse antigens, but not the docking orientation. *J. Immunol.* 181: 6255–6264.
25. Zhang, B., N. A. Bowerman, J. K. Salama, H. Schmidt, M. T. Spiotto, A. Schietinger, P. Yu, Y. X. Fu, R. R. Weichselbaum, D. A. Rowley, et al. 2007. Induced sensitization of tumor stroma leads to eradication of established cancer by T cells. *J. Exp. Med.* 204: 49–55.
26. Savage, P. A., J. J. Boniface, and M. M. Davis. 1999. A kinetic basis for T cell receptor repertoire selection during an immune response. *Immunity* 10: 485–492.
27. Rosette, C., G. Werlen, M. A. Daniels, P. O. Holman, S. M. Alam, P. J. Travers, N. R. Gascoigne, E. Palmer, and S. C. Jameson. 2001. The impact of duration versus extent of TCR occupancy on T cell activation: a revision of the kinetic proofreading model. *Immunity* 15: 59–70.
28. Daniels, M. A., E. Teixeiro, J. Gill, B. Hausmann, D. Roubaty, K. Holmberg, G. Werlen, G. A. Holländer, N. R. J. Gascoigne, and E. Palmer. 2006. Thymic selection threshold defined by compartmentalization of Ras/MAPK signalling. *Nature* 444: 724–729.
29. Eisen, H. N. 1974. *Immunology.* Harper & Row Publishers, Inc., Hagerstown, MD. p. 403.
30. Scatchard, G. 1949. The Attraction of Proteins for Small Molecules and Ions. *Ann. N. Y. Acad. Sci.* 51: 660–672.
31. Schreier, A. A., and P. R. Schimmel. 1974. Interaction of manganese with fragments, complementary fragment recombinations, and whole molecules of yeast phenylalanine specific transfer RNA. *J. Mol. Biol.* 86: 601–620.
32. Wooldridge, L., H. A. van den Berg, M. Glick, E. Gostick, B. Laugel, S. L. Hutchinson, A. Milicic, J. M. Brenchley, D. C. Douek, D. A. Price, and A. K. Sewell. 2005. Interaction between the CD8 coreceptor and major histocompatibility complex class I stabilizes T cell receptor-antigen complexes at the cell surface. *J. Biol. Chem.* 280: 27491–27501.
33. Anikeeva, N., T. Mareeva, W. Liu, and Y. Sykulev. 2009. Can oligomeric T-cell receptor be used as a tool to detect viral peptide epitopes on infected cells? *Clin. Immunol.* 130: 98–109.
34. Cameron, T. O., P. J. Norris, A. Patel, C. Moulon, E. S. Rosenberg, E. D. Mellins, L. R. Wedderburn, and L. J. Stern. 2002. Labeling antigen-specific CD4(+) T cells with class II MHC oligomers. *J. Immunol. Methods* 268: 51–69.
35. Wang, R., K. Natarajan, and D. H. Margulies. 2009. Structural basis of the CD8 alpha beta/MHC class I interaction: focused recognition orients CD8 beta to a T cell proximal position. *J. Immunol.* 183: 2554–2564.
36. Call, M. E., J. Pyrdol, M. Wiedmann, and K. W. Wucherpfennig. 2002. The organizing principle in the formation of the T cell receptor-CD3 complex. *Cell* 111: 967–979.
37. Fernández-Miguel, G., B. Alarcón, A. Iglesias, H. Bluethmann, M. Alvarez-Mon, E. Sanz, and A. de la Hera. 1999. Multivalent structure of an alphabetaT cell receptor. *Proc. Natl. Acad. Sci. USA* 96: 1547–1552.
38. Kuhns, M. S., A. T. Girvin, L. O. Klein, R. Chen, K. D. Jensen, E. W. Newell, J. B. Huppa, B. F. Lillemeier, M. Huse, Y. H. Chien, et al. 2010. Evidence for a functional sidedness to the alphabetaTCR. *Proc. Natl. Acad. Sci. USA* 107: 5094–5099.
39. Schrum, A. G., D. Gil, L. A. Turka, and E. Palmer. 2011. Physical and functional bivalency observed among TCR/CD3 complexes isolated from primary T cells. *J. Immunol.* 187: 870–878.
40. Campi, G., R. Varma, and M. L. Dustin. 2005. Actin and agonist MHC-peptide complex-dependent T cell receptor microclusters as scaffolds for signaling. *J. Exp. Med.* 202: 1031–1036.
41. Schamel, W. W., I. Arechaga, R. M. Risueño, H. M. van Santen, P. Cabezas, C. Risco, J. M. Valpuesta, and B. Alarcón. 2005. Coexistence of multivalent and monovalent TCRs explains high sensitivity and wide range of response. *J. Exp. Med.* 202: 493–503.
42. Carpentier, B., P. Pierobon, C. Hivroz, and N. Henry. 2009. T-cell artificial focal triggering tools: linking surface interactions with cell response. *PLoS ONE* 4: e4784.
43. Alexander, E. L., and B. Wetzel. 1975. Human lymphocytes: similarity of B and T cell surface morphology. *Science* 188: 732–734.
44. Hartman, N. C., and J. T. Groves. 2011. Signaling clusters in the cell membrane. *Curr. Opin. Cell Biol.* 23: 370–376.
45. Hornick, C. L., and F. Karush. 1969. The interaction of hapten-coupled bacteriophage phi-X-174 with antihapten antibody. *Isr. J. Med. Sci.* 5: 163–170.
46. Artyomov, M. N., M. Lis, S. Devadas, M. M. Davis, and A. K. Chakraborty. 2010. CD4 and CD8 binding to MHC molecules primarily acts to enhance Lck delivery. *Proc. Natl. Acad. Sci. USA* 107: 16916–16921.
47. Xiong, Y., P. Kern, H. Chang, and E. Reinherz. 2001. T Cell Receptor Binding to a pMHCII Ligand Is Kinetically Distinct from and Independent of CD4. *J. Biol. Chem.* 276: 5659–5667.
48. Hendrickson, W. A., A. Pähler, J. L. Smith, Y. Satow, E. A. Merritt, and R. P. Phizackerley. 1989. Crystal structure of core streptavidin determined from multiwavelength anomalous diffraction of synchrotron radiation. *Proc. Natl. Acad. Sci. USA* 86: 2190–2194.
49. Edidin, M. 2003. The state of lipid rafts: from model membranes to cells. *Annu. Rev. Biophys. Biomol. Struct.* 32: 257–283.
50. Lillemeier, B. F., M. A. Mörtelmaier, M. B. Forstner, J. B. Huppa, J. T. Groves, and M. M. Davis. 2010. TCR and Lat are expressed on separate protein islands on T cell membranes and concatenate during activation. *Nat. Immunol.* 11: 90–96.
51. Lillemeier, B. F., J. R. Pfeiffer, Z. Surviladze, B. S. Wilson, and M. M. Davis. 2006. Plasma membrane-associated proteins are clustered into islands attached to the cytoskeleton. *Proc. Natl. Acad. Sci. USA* 103: 18992–18997.
52. Levental, I., M. Grzybek, and K. Simons. 2010. Greasing their way: lipid modifications determine protein association with membrane rafts. *Biochemistry* 49: 6305–6316.
53. Cho, B. K., K. C. Lian, P. Lee, A. Brunmark, C. McKinley, J. Chen, D. M. Kranz, and H. N. Eisen. 2001. Differences in antigen recognition and cytolytic activity of CD8(+) and CD8(-) T cells that express the same antigen-specific receptor. *Proc. Natl. Acad. Sci. USA* 98: 1723–1727.
54. Sykulev, Y., Y. Vugmeyster, A. Brunmark, H. L. Ploegh, and H. N. Eisen. 1998. Peptide antagonism and T cell receptor interactions with peptide-MHC complexes. *Immunity* 9: 475–83.